

**Memory effects in strongly interacting lattice gases: Self-intermediate scattering function studies**L. Skarpalezos,<sup>\*</sup> N. Tsakiris, and P. Argyrakis<sup>†</sup>*Physics Department, University of Thessaloniki, GR-54124 Thessaloniki, Greece*

V. S. Vikhrenko

*Belarusian State Technological University, 13a Sverdlova Str., BY-220006 Minsk, Belarus*

(Received 18 March 2011; revised manuscript received 23 June 2011; published 12 August 2011)

We investigate in detail the self-intermediate scattering function (SISF) of a lattice fluid (interacting lattice gas) with attractive nearest-neighbor interparticle interactions at a temperature slightly above the critical one by means of Monte Carlo simulations. An analytical expression is suggested to reproduce the simulation data. This expression is the generalization of the hydrodynamic limit with the wave vector, the time-dependent tracer diffusion coefficient, and the lattice geometry factor, instead of the square of the wave vector. The tracer diffusion coefficient is given by its zero wave-vector limit multiplied by the exponent of a function that contains only one fitting parameter describing its wave-vector dependence. In order to represent the time dependence of the SISF and to understand the time scales of the lattice fluid relaxation processes, we use two- and three-exponential fitting functions. The relaxation times group in three well-separated regions around 10, 100, and 1000 Monte Carlo steps and show weak concentration dependence. The analytical expression can also be used to calculate the lattice fluid dynamical structure factor.

DOI: [10.1103/PhysRevB.84.075476](https://doi.org/10.1103/PhysRevB.84.075476)

PACS number(s): 66.30.-h, 68.43.De

**I. INTRODUCTION**

Lattice systems have played a very important role in understanding phase-transition phenomena,<sup>1–3</sup> and they are frequently used as simplified (lattice gas) models for a number of real objects: submonolayers on solid surfaces,<sup>4,5</sup> ionic crystals,<sup>6</sup> intercalation compounds,<sup>7,8</sup> electrons on traps,<sup>9</sup> etc. The most important applications deal with lattice-gas transport processes, mostly diffusion processes.<sup>4,5,9–14</sup> Linear response considerations<sup>15,16</sup> offer a straightforward way for investigating kinetic transport coefficients, and they have been applied in the past for investigating lattice-gas diffusion characteristics.<sup>10,14,17,18</sup>

On the other hand, the space- and time-dependent density-density distribution functions, their spatial Fourier and time Laplace transforms, the intermediate scattering functions (ISF), and the dynamical structure factors (DSF), they all contain valuable information about kinetic properties of the matter in a wide range of spatial and time scales. Dynamical structure factors and intermediate scattering functions of different liquids and fluids as well as lattice-gas automata have been intensively investigated in the past,<sup>19–25</sup> while for lattice gases the corresponding data are rather scarce (lattice fluids is a more appropriate term because a wide range of particle densities up to liquid values are considered).<sup>26–28</sup>

Moreover, up to now, lattice gases have been investigated but only without lateral interactions. The influence of intrasite particle dynamics (its hindered oscillatory motion near the lattice site and the possibility to make long jumps depending on the friction constant) on the DSF of a single particle on one- and two-dimensional lattices has been investigated.<sup>29,30</sup> The evolution of the structure factor during the first-order phase transition in the lattice system was used to extract diffusion coefficients at nonequilibrium conditions.<sup>31</sup> Several theories for ISF have been developed<sup>32–35</sup> that lead to very accurate results for the long time and small wave-vector tracer diffusion coefficient in the entire concentration range, however, their

consequences in the nonhydrodynamic regimes have not been investigated.

At the same time, in many cases<sup>21,36–39</sup> the diffusion process in liquids is considered as a combination of smooth particle motion together with its surrounding ones and of sudden particle jumps between “free” volumes<sup>40</sup> created by the surrounding particles. Many expressions for the tracer diffusion wave-vector dependence have been suggested to estimate the contribution of particle jumps in the diffusion process and to evaluate the jump parameters (e.g., the residence time and jump distances). However, no thorough investigation of the wave-vector dependence on the jumping mechanisms exists up to now. Memory effects have not been investigated as well.<sup>14,41</sup>

The self-intermediate scattering function (SISF) of noninteracting lattice gases was investigated<sup>27</sup> by Monte Carlo simulation techniques in a wide coverage range in the interval from 0.0998 up to 0.9805, and it was shown that memory effects are quite significant. It was shown that the Bardeen-Herring mechanism that explains interparticle correlations by movement of the “special vacancy” (this vacancy is created by a jumping particle that increases the probability for it to return to its original position<sup>27</sup>) and gives possibility to reproduce the long-time tracer diffusion can not explain satisfactorily the wave vector and time dependence of the SISF. In fact, no theoretical explanation for the simulation results has been provided. This is in spite of the fact that rather large square lattices (600 × 600 lattice sites) have been utilized, but the investigation was restricted to only 20 to 200 Monte Carlo steps (MCS), depending on particle concentration. As particles during this time can only move to a few lattice spacings, we can readily see that the lattice size has no crucial importance, while as it will be shown below the long-time behavior of interacting lattice fluids is of great importance. In simplified kinetic theories,<sup>42</sup> some improvements in the description of the SISF of noninteracting lattice gases were achieved,<sup>28</sup> however, time scales of the memory effects were not discussed.

We present here the results of Monte Carlo simulations and the calculation of the SISF for the lattice fluid with nearest-neighbor attractive interactions for long (up to 2000 MCS) times at two temperatures slightly above the critical one (where interparticle interactions strongly manifest themselves). Emphasis is given to the self-intermediate scattering function  $F_s(\mathbf{k}, t)$  that is closely related to the tracer diffusion in the lattice fluid. Approximate expressions for the wave vector and time dependence of SISF are suggested, and the time dependence of its parameters is investigated in detail. The wave-vector dependence is described by only one fitting parameter, and the suggested expression reproduces well the simulation results for different orientations of the wave vector. With these expressions the dynamical structure factor can be calculated in a straightforward manner.

## II. THEORETICAL BACKGROUND

The van Hove space- and time-dependent distribution function can be represented by the expression:

$$G(\mathbf{r}, t) = \frac{1}{n} \left\langle \sum_{i,j=1}^n \delta[\mathbf{r} + \mathbf{r}_i(0) - \mathbf{r}_j(t)] \right\rangle = G_s(\mathbf{r}, t) + G_d(\mathbf{r}, t), \quad (1)$$

where  $\delta(\mathbf{r})$  is Dirac's  $\delta$  function,  $\mathbf{r}$  is a radius vector,  $t$  is time, and the angular brackets mean averaging over canonical ensemble of  $n$  particles. The sum runs over positions of all system particles denoted by radius vectors  $\mathbf{r}_i$  and  $\mathbf{r}_j$ . For lattice fluids, particles can occupy the lattice sites only. Two- and many-particle occupation of a lattice site is forbidden. The self part  $G_s(\mathbf{r}, t)$  of the distribution function contains positions of the same particle ( $i = j$ ) at two different times (0 and  $t$ ), while the distinct part  $G_d(\mathbf{r}, t)$  contains the terms with  $i \neq j$ .

In the hydrodynamic limit of long distances and times, the self part of the distribution function obeys the diffusion equation:

$$\frac{\partial G_s(\mathbf{r}, t)}{\partial t} = \nabla \cdot [\mathbf{D}_s \cdot \nabla G_s(\mathbf{r}, t)], \quad (2)$$

where  $D_s$  is the self- (or tracer) diffusion tensor.

The self-intermediate scattering function (SISF)  $F_s(\mathbf{k}, t)$  is the Fourier transform of the self part of the distribution function. Because for a lattice fluid the initial conditions are taken in the form  $G_s(0, 0) = 1$  and  $G_s(\mathbf{r} \neq 0, 0) = 0$ , and from Eq. (2) it follows that

$$F_s(\mathbf{k}, t) = \exp(-\mathbf{k} \cdot \mathbf{D}_s \cdot \mathbf{k} t), \quad (3)$$

where  $\mathbf{k}$  is the wave vector. The tracer diffusion tensor  $\mathbf{D}_s$  in the hydrodynamic limit does not depend on the wave vector and time. In this case, the SISF is a Gaussian in  $\mathbf{k}$  space with decreasing half-width inversely proportionally to square root of time. For lattices of cubic symmetry, the tracer diffusion tensor reduces to the tracer diffusion coefficient that can be calculated through the self-intermediate scattering function

$$D_s = -\frac{\ln[F_s(k, t)]}{k^2 t}. \quad (4)$$

However, the lattice fluid dynamics is governed by the master equation and the solution (3) and expression (4) can not

be used in the region of large wave vectors and short times. For a particle on the lattice of cubic symmetry when considering its uncorrelated jumps to the nearest-neighbor sites<sup>37</sup> as well as for the lattice fluid when memory effects can be neglected,<sup>41</sup> in Eq. (4),  $k^2$  has to be replaced by a function

$$\eta(\mathbf{k}) = \sum_{j=1}^z \frac{1 - \cos(\mathbf{k} \cdot \mathbf{r}_j)}{a^2}, \quad (5)$$

where the sum runs over  $z$  nearest-neighbor sites on the lattice. For a square lattice, it reduces to

$$\begin{aligned} \eta(\mathbf{k}) &= 2 \frac{2 - \cos(k_x a) - \cos(k_y a)}{a^2} \\ &= \frac{4}{a^2} \left[ \sin^2\left(\frac{k_x a}{2}\right) + \sin^2\left(\frac{k_y a}{2}\right) \right], \end{aligned} \quad (6)$$

where  $a$  is the lattice spacing and  $x$  and  $y$  axes are directed along the cell edges.

When the memory effects are taken into account, the master equation requires considering next-nearest, next-next-nearest, and so on neighbors, and it is not possible to separate the lattice geometry contribution to the intermediate scattering function in a simple term such as Eq. (6).<sup>27</sup> Nevertheless, we preserve this simple equation for separating the lattice geometry contribution because at small  $k$  it satisfies the hydrodynamic limit, and moreover, it is a periodic function of the wave vector with a period equal to the first-Brillouin-zone size.

All other contributions of the memory effects to  $F_s(\mathbf{k}, t)$  are included through the time and wave-vector dependence of the tracer diffusion coefficient

$$F_s(\mathbf{k}, t) = \exp[-D_s(\mathbf{k}, t)\eta(\mathbf{k})t]. \quad (7)$$

Thus Eq. (4) can be rewritten as

$$D_s(\mathbf{k}, t) = -\frac{\ln[F_s(\mathbf{k}, t)]}{\eta(\mathbf{k})t}. \quad (8)$$

Indeed, at small  $k$ , Eqs. (4) and (8) coincide with each other.

In accordance with Eqs. (3), (4) and (7), (8), the logarithm of the SISF decreases inversely proportionally with time. In the hydrodynamic regime ( $t \rightarrow \infty, k \rightarrow 0$ ) when the tracer diffusion coefficient is a constant, SISF decreases exponentially with time

$$F_s(t) = \exp\left(-\frac{t}{\tau}\right), \quad (9)$$

with the relaxation time  $\tau = \tau(k) = [D_s k^2]^{-1}$  increasing inversely proportionally with  $k^2$  when  $k \rightarrow 0$ .

However, even for a single particle on a lattice, this dependence is violated at short times due to the nonzero probability for the particle to return to its original position.<sup>43</sup> The time dependence of the diffusion coefficient can reflect memory effects of the diffusion process. At nonzero concentration, memory effects significantly modify the diffusion-coefficient time dependence. Moreover, in general, the diffusion coefficient as defined by Eq. (8) depends on the wave vector. In the following, Eq. (8) is used for calculating the diffusion coefficient as a function of  $t$  and  $\mathbf{k}$  and for the analysis of the memory effects.

### III. SIMULATION PROCEDURES

The initial configuration we used for the Monte Carlo simulations was a square ( $L \times L = 50 \times 50$ ) lattice with periodic boundary conditions randomly occupied by particles with a coverage (concentration)  $\theta$ . In this case, the wave vector

$$\mathbf{k} = \frac{2\pi}{La} (h\mathbf{i} + m\mathbf{j}), \quad h, m = 0, 1, 2, \dots, \frac{L}{2}, \quad h + m \neq 0, \quad (10)$$

is introduced. Here,  $\mathbf{i}$  and  $\mathbf{j}$  are the unit vectors in the  $x$  and  $y$  direction, respectively.

We then applied attractive nearest-neighbor interactions between the particles using the following algorithm: the probability  $p$  of a randomly chosen particle to jump to a nearest-neighbor empty site depends on the number of nearest neighbors  $z$  and on temperature  $T$  of the system by the following expression:

$$p = \exp(-zJ/k_B T), \quad (11)$$

where  $J$  is the interaction parameter, which is linked to the critical temperature by the relation  $J/(k_B T_c) \cong 1.76$ , and  $k_B$  is the Boltzmann constant.

MCS is then defined by  $n = \theta \times L \times L$  trials to move a randomly chosen particle. We let the system evolve until it reaches an equilibrium state ( $10^4$  MCS) before starting to compute at each MCS the value of the self-intermediate scattering function  $F_s(\mathbf{k}, t)$  for a time range of 2000 MCS. In fact, we considered the equilibrium state as the initial state for our calculations ( $t_0 = 0$ ). Afterward, by tracking the position  $(x_i, y_i)$  of every particle at every time step,  $F_s(\mathbf{k}, t)$  was easily computed for all the wave vectors  $k_x = 2\pi h/La$  and  $k_y = 2\pi m/La$ :

$$F_s(\mathbf{k}, t) = \frac{1}{n} \sum_i^n \cos \left\{ \frac{2\pi}{L} [h(x_{i,t} - x_{i,0}) + m(y_{i,t} - y_{i,0})] \right\}, \quad (12)$$

where  $h$  and  $m$  are two integers varying independently from 0 to  $L/2$  (for symmetry reasons the negative values were not considered) and the particle coordinates are given in units of  $a$ . The results obtained are the average of 20 000 independent runs.

Simulations were performed for two temperatures slightly above the critical value ( $T = 1.05T_c$  and  $T = 1.2T_c$ ) and for the concentration range  $\theta$  from 0.3 to 0.7 with a step 0.05. The lattice spacing  $a$  was taken equal to 1.

### IV. RESULTS AND DISCUSSION

The simulation results for the SISF are shown in Fig. 1(a). The width of the function in  $k$  space decreases with time as given by Eqs. (3) and (7), as is always observed in experiments and simulations for liquids and lattice fluids. Figure 1(b) demonstrates that the tracer diffusion coefficient sharply decreases with  $k$  in the region of small  $k$ , and then decreases more slowly when  $k$  is approaching the boundary of the first Brillouin zone. The tangents are horizontal at  $k = 0$  and  $k = k_m$ , where  $k_m = \pi/a$  is the maximal wave-vector value (we first consider the results for  $\mathbf{k}$  directed along a cell

edge). Thus it is reasonable to approximate the simulation data by the expression

$$D_s(k, t) = D_{s0}(t) \exp[-B^2(k, t)], \quad (13)$$

where  $B(0, t) = 0$  and the first derivative of  $B(k, t)$  over the wave vector at the boundary of the first Brillouin zone is equal to zero as well.

To gain understanding on how to approximate the diffusion coefficient simulation data, we calculated the function  $B(k, t) = \sqrt{\ln [D_{s0}/D_s(k, t)]}$ . Typical results are given in Fig. 1(c). The function is exponentially increasing to its saturation value. However, to guarantee zero value of its first derivative at the boundary of the first Brillouin zone, we have introduced the first-order term in  $k$ , and the final expressions now have the forms

$$B(k, t) = b(\xi)B_m(t), \quad B_m(t) = B(\xi_m, t), \quad (14)$$

$$\xi = h/\kappa(t), \quad \xi_m = 25/\kappa(t),$$

$$b(\xi) = b_0[1 - \exp(-\xi) - \xi \exp(-\xi_m)], \quad (15)$$

$$b_0 = 1/[1 - (1 + \xi_m) \exp(-\xi_m)],$$

where  $\xi$  is a dimensionless variable,  $h$  is considered as an integer varying between 0 and 25, and the characteristic distance  $\kappa$  in the inverse space is taken in units of  $(2\pi/La)$ . Also,  $b(k, t) = b(\xi)$  is a function of  $\xi$  that depends on time through the parameter  $\kappa$  only,  $b(0) = 0$ , and  $b(\xi_m) = 1$ . This function represents well the wave-vector dependence of the function  $B(k, t)$  [see Fig. 1(c)].

The pre-exponential factor in Eq. (13) is a limiting value

$$D_{s0}(t) = \lim_{k \rightarrow 0} D_s(k, t). \quad (16)$$

Since the values for  $k = 0$  are inaccessible in Monte Carlo simulations, the results for  $k = \pm 1$  and  $\pm 2$  were approximated by parabolas and the values of  $D_{s0}$  were calculated in this way.

Thus all simulation data can be approximated by three time-dependent parameters, namely,  $D_{s0}(t)$ ,  $B_m(t)$ , and  $\kappa(t)$ , where  $\kappa(t)$  is the only fitting parameter representing the  $k$ -space dependence. All these functions can in turn be approximated by a two- or three-exponential fitting, providing good understanding of the time scales of the memory effects.

The existence of memory effects and asymptotic exponential time dependence of the intermediate scattering function was demonstrated for lattice gases with repulsive nearest-neighbor interactions.<sup>44</sup> However, the short-time memory effects have not been investigated in detail. Our results are quite adequately represented by the expressions:

$$D_{s0}(t) = D_\infty + D_1 \exp(-t/\tau_1) + D_2 \exp(-t/\tau_2), \quad (17)$$

$$\kappa(t) = \kappa_\infty + \kappa_1 \exp(-t/\tau_{\kappa 1}) + \kappa_2 \exp(-t/\tau_{\kappa 2}) + \kappa_3 \exp(-t/\tau_{\kappa 3}), \quad (18)$$

$$B_m(t) = B_\infty + B_1 \exp(-t/\tau_{b1}) + B_2 \exp(-t/\tau_{b2}) + B_3 \exp(-t/\tau_{b3}). \quad (19)$$

It is worth noting here that the relaxation times do not depend on the absolute value of the wave vector. The

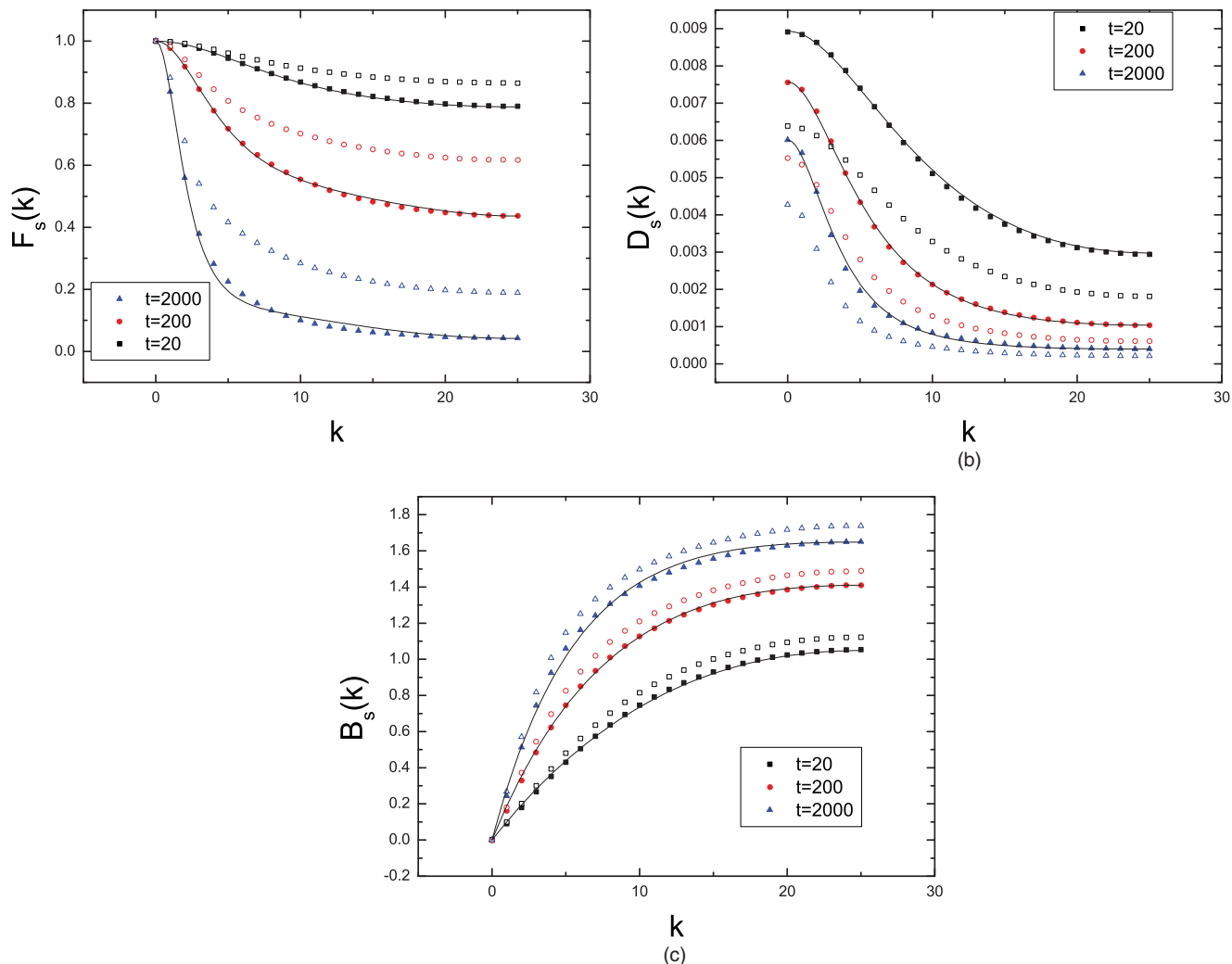


FIG. 1. (Color online) (a) The SIF, (b) the tracer diffusion coefficient, and (c) function  $B$  vs the wave vector directed along a cell edge for three different times.  $\theta = 0.5$ ,  $T = 1.2T_c$  (full symbols), and  $T = 1.05T_c$  (empty symbols). Time  $t$  is given in MCS. Solid lines are drawn according to Eqs. (7) and (13)–(19) only for the data of  $T = 1.2T_c$  and not for  $T = 1.05T_c$  (for clarity in the figures).

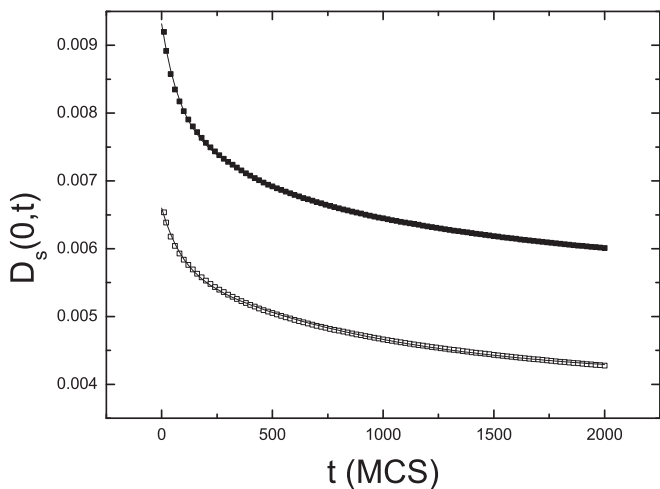


FIG. 2. The tracer diffusion coefficient at  $k = 0$  vs time.  $\theta = 0.5$ ,  $T = 1.2T_c$  (full symbols), and  $T = 1.05T_c$  (empty symbols). Solid lines for the two temperatures are drawn according to Eq. (17).

wave-vector dependence of the relaxation process is mainly manifested through the scaling parameter  $\kappa$ . One can see from Fig. 1 that Eqs. (7) and (13)–(19) agree quite well with the simulation results even at long times, as long as 2000 MCS.

The time dependence of  $D_{s,0}$  is shown in Fig. 2. It is well represented by the two-exponential decay function (17). The pre-exponential factors and the relaxation times for different concentrations are presented in Figs. 3(a) and 3(b), respectively. The parameters of the scaling factor  $\kappa$  in the wave-vector space and function  $B_m$  are shown in Figs. 4(a), 4(b) and 5(a), 5(b) correspondingly.

All relaxation times fall into three well-separated intervals: 5 to 18, 50 to 120, and 500 to 1000 MCS. If we look at each of the three parameters individually, the separation of relaxation times is even more pronounced with time values separated by approximately one order of magnitude. The concentration dependence of the relaxation times for all three parameters is rather weak.

The pre-exponential factors of the long wavelength limit of the tracer diffusion coefficient strongly decrease with

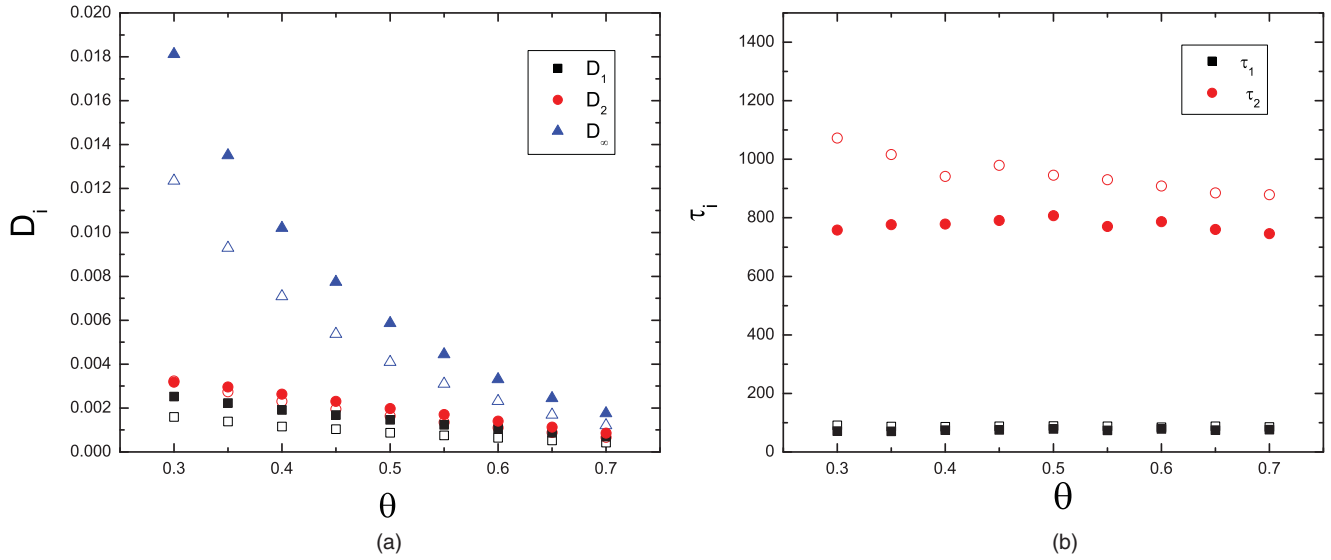


FIG. 3. (Color online) (a) The pre-exponential coefficients and (b) the relaxation times for the tracer diffusion coefficient as given by Eq. (17) at  $k = 0$  vs lattice concentration.  $T = 1.2T_c$  (full symbols) and  $T = 1.05T_c$  (empty symbols).

concentration [see Fig. 3(a)] unlike the relaxation times, which remain approximately constant or slightly decrease [see Fig. 3(b)]. The pre-exponential factors of the scaling factor  $\kappa$  strongly increase with concentration [see Fig. 4(a)] while its relaxation times slightly decrease [see Fig. 4(b)]. Concerning function  $B_m$ , the pre-exponential factors decrease significantly [see Fig. 5(a)] while the relaxation times do not vary with concentration [see Fig. 5(b)]. The contribution of the relaxation processes in the regions of tens and hundreds of MCS are approximately equal, while the scaling factor  $\kappa$  strongly relaxes on the time scale of 5 MCS. Such a behavior of the relaxation times is rather unexpected because at larger concentration, particle jumps become less frequent and more time is necessary for particle-distribution evolution. However, this dependence of SISF relaxation on particle jump

frequencies [which is inversely proportional to  $D_s(k,t)$  and follows from Eqs. (7) and (9)] is not related to memory effects, and therefore, we have used the analysis of the diffusion coefficient itself. One can also explain this effect by considering the movement of the special vacancy,<sup>27</sup> which reduces the long-time particle mobility without contributing to the memory effects.

For symmetry reasons, it is sufficient to consider 1/8 part of the first Brillouin zone between its diagonal and  $x$  axes for other orientations of the wave vector. Then all expressions (12) through (18) can be used replacing  $k$  with  $k_x$ , the projection of  $\mathbf{k}$  on  $x$ . The anisotropy of the SISF is manifested through the dependence of the pre-exponential factors and the relaxation times in Eqs. (16) through (18) on  $k_y$  or the angle between  $\mathbf{k}$  and  $x$  axes. The anisotropy for the relaxation times is not very

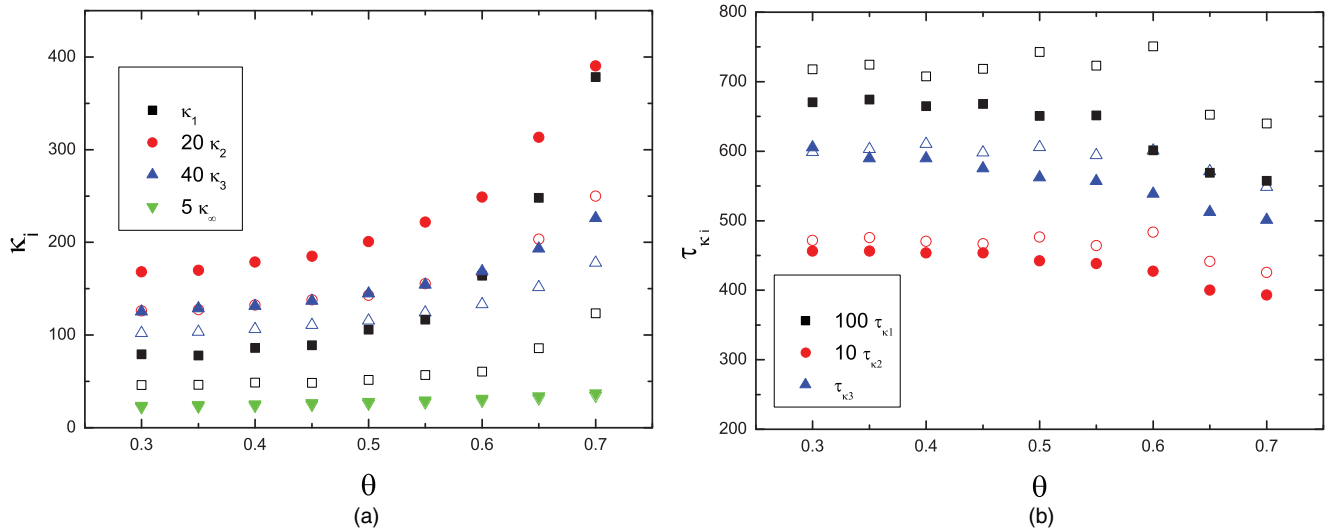


FIG. 4. (Color online) (a) The pre-exponential coefficients and (b) the relaxation times for the characteristic distance  $\kappa$  in the inverse space as given by Eq. (18) vs lattice concentration for the wave vector directed along a cell edge.  $T = 1.2T_c$  (full symbols) and  $T = 1.05T_c$  (empty symbols).

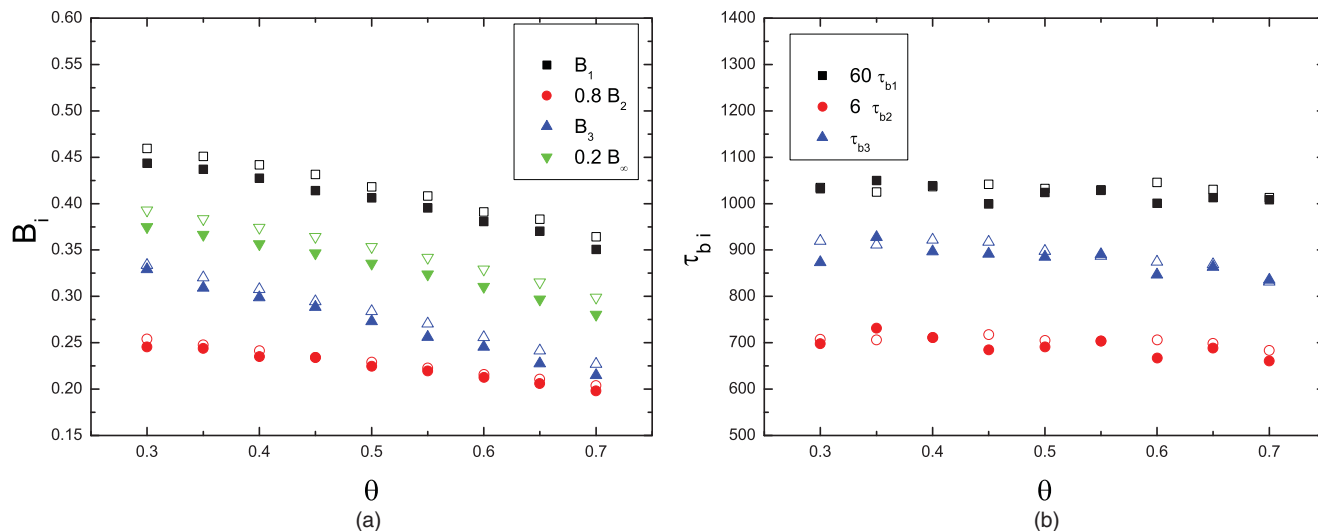


FIG. 5. (Color online) (a) The pre-exponential coefficients and (b) the relaxation times for  $B_m$  as given by Eq. (19) vs lattice concentration for the wave vector directed along a cell edge.  $T = 1.2T_c$  (full symbols) and  $T = 1.05T_c$  (empty symbols).

strong and amounts to a few tenths of the values for  $\mathbf{k}$  oriented along a cell edge. An example is given in Fig. 6, where the parameters of the scaling factor  $\kappa$  are shown for the diagonal orientation of the wave vector.

The depth of relaxation can be estimated as the ratio of the difference between the initial and final (at  $t \rightarrow \infty$ ) parameter values to its final value. The results are represented in Fig. 7. At  $T = 1.2T_c$ , the depth of relaxation of the tracer diffusion coefficient at  $k = 0$  changes almost linearly with concentration from approximately 0.3 to 0.9 for  $\mathbf{k}$  oriented along a cell edge, and from approximately 0.45 to 0.9 for diagonal orientation. The strongest relaxation is observed for the scaling parameter  $\kappa$ . With concentration increase, it increases approximately from 19 to 54, and from 5.7 to 7.7 for wave-vector orientations along the cell edge and diagonal,

correspondingly. Thus the depth of relaxation of the scaling parameter is strongly anisotropic in the wave-vector space. At  $T = 1.05T_c$ , this increase is not so strong and for the cell-edge wave-vector orientation it changes from approximately 12 to 20. The depth of  $B_m$  relaxation is modest and is approximately 0.6 and 0.5, independently of concentration and temperature, for wave-vector orientations along the cell edge and diagonal, respectively.

Thus the anisotropy of the memory effects is clearly seen especially for the scaling parameter  $\kappa$ . However, as the scaling parameter initially sharply decreases with time from its large values ( $\kappa_1$  considerably exceeds all the other pre-exponential factors) the anisotropy of its depth of relaxation is probably overestimated. Its short-time behavior has to be additionally investigated in more detail. Also, it is necessary to note that

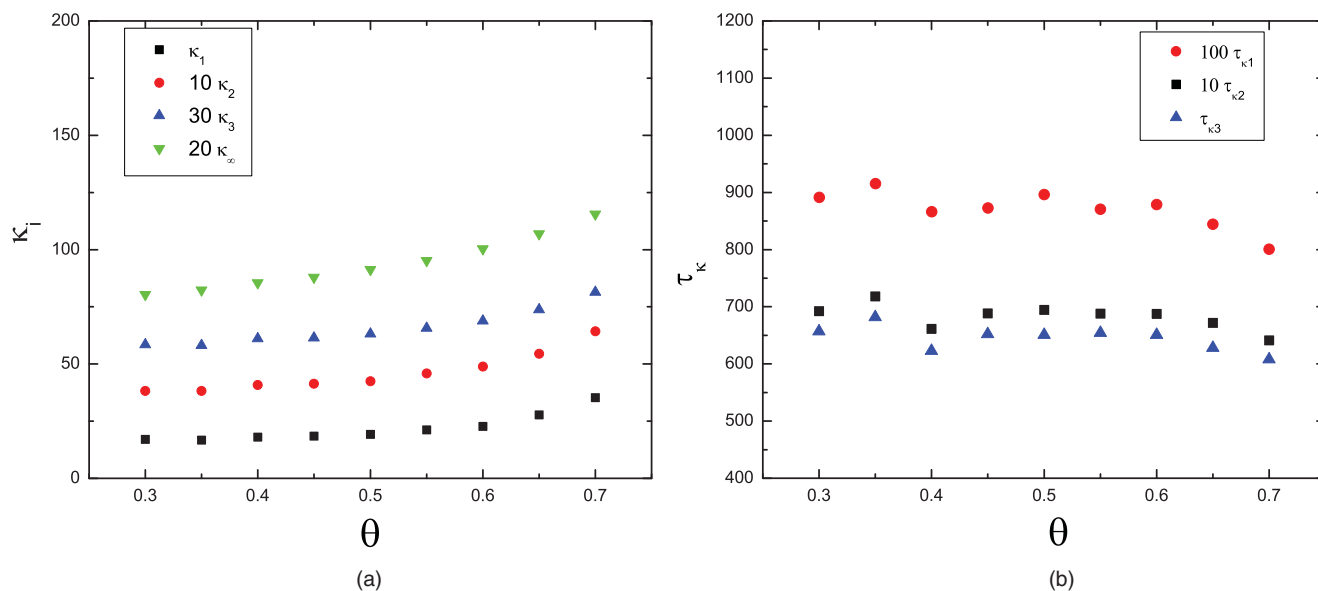


FIG. 6. (Color online) (a) The pre-exponential coefficients and (b) the relaxation times for the characteristic distance  $\kappa$  in the inverse space as given by Eq. (17) vs lattice concentration for the wave vector directed along a cell diagonal.  $T = 1.2T_c$ .

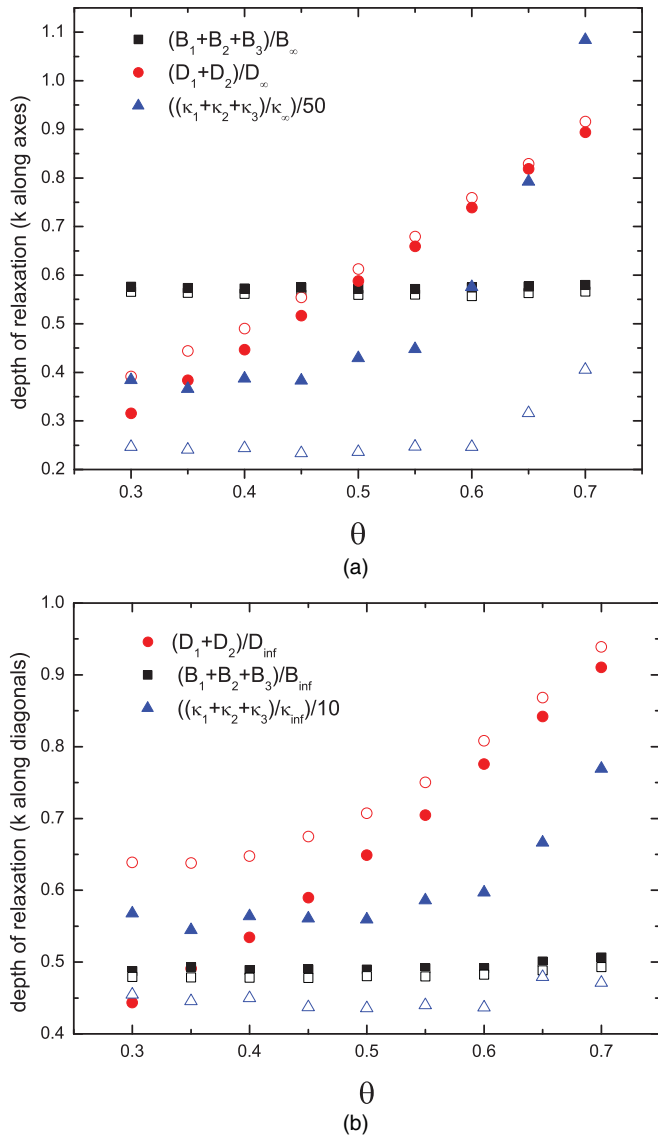


FIG. 7. (Color online) The depth of relaxation for the parameters  $D_{s0}$ ,  $B_m$ , and  $\kappa$  vs lattice concentration for (a) the wave vector directed along a cell axis and for (b) the wave vector directed along a cell diagonal.  $T = 1.2T_c$  (full symbols) and  $T = 1.05T_c$  (empty symbols).

the size of the lattice considered ( $L = 50$ ) is not large enough to adequately represent the hydrodynamic limit  $k \rightarrow 0$ . The tracer diffusion coefficient at  $k = 0$  must be independent of the wave-vector orientation. Its small anisotropy in our simulations is the result of not large enough lattice size.

Comparing the results for two temperatures ( $T = 1.2T_c$  and  $T = 1.05T_c$ ), we see that the difference between them is not very pronounced except for the tracer diffusion coefficient in the long-wavelength limit. Due to lower  $D_{s0}$  values for the case of  $T = 1.05T_c$ , the SISF decreases less abruptly with  $k$  than for  $T = 1.2T_c$ . The dependence of the various parameters (pre-exponential factors and relaxation times) of  $D_{s0}$ ,  $B_m$ , and  $\kappa$  on concentration follow similar behavior for both temperatures. For the lower temperature, the pre-exponential factors of  $D_{s0}$  are shifted to smaller values (by some 30%), while the relaxation times to larger ones (appreciatively 15%

increase). For  $B_m$ , the pre-exponential factors are shifted to larger values while the relaxation times remain the same. Concerning  $\kappa$ , the pre-exponential factors are shifted to smaller values and their increase with coverage is less abrupt, while the relaxation times are shifted to a somewhat larger values and this behavior correlates well with their concentration dependence. The depth of relaxation of the tracer diffusion coefficient at  $k = 0$  seems to change linearly for  $T = 1.2T_c$  but this is not the case for  $T = 1.05T_c$ .

At the same time, for a noninteracting lattice gas that can be considered as a limiting high-temperature case the relaxation times are considerably shorter and do not exceed 20 MCS<sup>27</sup> for the concentration range of  $\theta = 0.3$ – $0.7$ . However, the authors of that work analyzed the logarithm of SISF (not the diffusion coefficient as done in the present work). This means that the direct proportionality of the logarithm of SISF to time as it is indicated by Eqs. (7) and (9) has not been separated in the analysis and their results cannot be directly compared with ours.

Considering the results represented by Eqs. (7)–(9) and (13)–(19) and Figs. 1–8, we have to note that the time dependence of SISF is very complicated. The main hydrodynamic trend that is given in Eq. (9) does not capture the memory effects caused by the complicated hopping dynamics of particles. These effects reveal themselves through the wave-vector-dependent tracer diffusion coefficient. There are two major relaxation times describing the zero wave-vector diffusion-coefficient evolution in accordance with Eq. (17). The other relaxation times are superimposed on these two relaxation scales in accordance with Eq. (13). They describe complicated evolution of the diffusion coefficient in the inverse  $k$  space. In fact, this evolution cannot be described by exponentially decaying functions because Eq. (13) contains the exponent of squared function  $B$ , the time dependence of which is given by a succession of relaxation functions in Eq. (19) and even more complicated time dependence through the inverse-space scaling factor  $\kappa$  in Eqs. (14) and (15).

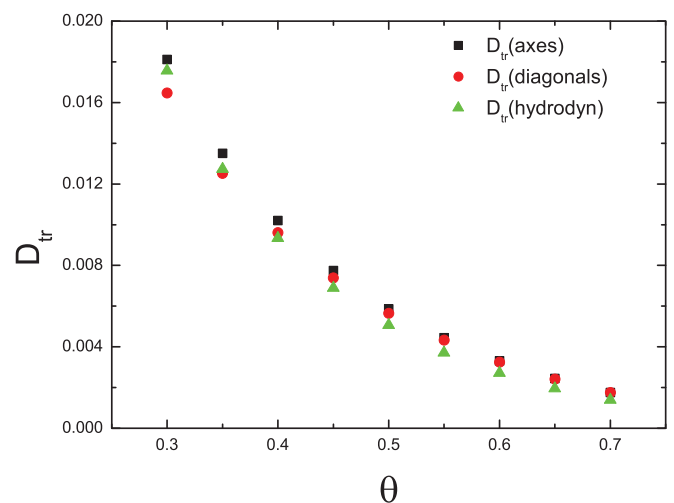


FIG. 8. (Color online) Comparison of the hydrodynamic value of the tracer diffusion coefficient (at  $k = 0$  and  $t \rightarrow \infty$ ) obtained after 2000 MCS with the results of Monte Carlo simulations through the particle mean-square displacement obtained after 10 000 MCS.  $T = 1.2T_c$ .

In Fig. 8, the hydrodynamic value of the tracer diffusion coefficient (at  $k = 0$  and  $t \rightarrow \infty$ ) is compared with the results of Monte Carlo simulations through the particle mean-square displacement as given by the expression

$$\langle(\Delta r)^2\rangle = 4D_{\text{tr}0}t, \quad (20)$$

where the time is given in MCS and the mean-square displacement in squared lattice spacing.

The difference between its values for the wave-vector orientations along the cell edge and diagonal is the result of not large enough lattice size, and partly due to inadequate statistics at low coverage. The values calculated from Eq. (20) are systematically slightly below the values obtained from the analysis of the ISSF. The reason for this discrepancy is that the particle mean-square displacements were considered during runs of 10 000 MCS after 10 000 MCS for the system equilibration, while the SISF data were obtained from 2000 MCS runs after the same period of equilibration. The three-exponential fitting of the latter results reduces the difference only slightly, while it shows rather long additional relaxation time around 1180 MCS for  $\theta = 0.5$  and 1070 for  $\theta = 0.6$ . However, if the runs for the mean-square displacements are restricted to 2000 MCS, the difference between the results does not exceed 3% at large coverage. Thus to get more precise results for SISF, it is necessary to produce runs of 10 000 MCS.

## V. CONCLUSION

The simulation results for the self-intermediate scattering function (SISF) for a system of interacting particles in a two-dimensional surface are given by a simple analytical expression with only one fitting parameter for representing its wave-vector dependence. This expression can be used for simple calculation of the self part of the dynamical structure factor because its direct evaluation through Monte Carlo simulation is computer-time demanding.

The SISF expression brings valuable information about relaxation processes in lattice fluids. The expression consists of generalization of the tracer diffusion coefficient that depends on the wave vector and time. In turn, the latter is represented as the zero wave-vector time-dependent tracer diffusion coefficient  $D_{s0}(t)$  times the exponent of function  $-B^2(\mathbf{k}, t)$  that contains the SISF wave vector and time dependence as well. The wave-vector dependence of function  $B$  is represented by its value  $B_m$  at the boundary of the first Brillouin zone times a function of  $k$  that contains only one fitting parameter  $\kappa$ .

The time dependence of  $D_{s0}(t)$ ,  $B_m(t)$ , and  $\kappa(t)$  gives valuable information about the relaxation processes. The relaxation times are introduced in a way that they do not depend on absolute value of the wave vector. At  $T = 1.2T_c$ , the relaxation of the zero wave-vector tracer diffusion coefficient is described by two relaxation times around 75 and 750 MCS that are almost independent of the concentration. The partial contributions of these relaxation processes are approximately equal in the entire concentration range 0.3–0.7 considered.  $B_m$  shows three relaxation times around 17, 110, and 900 MCS, again without pronounced concentration dependence. The three relaxation times of  $\kappa$  slightly decrease in ranges of 6 to 5, 60 to 50, and 670 to 560 MCS with concentration increase from 0.3 to 0.7. At the lower temperature of  $1.05T_c$ , all the parameters show similar concentration dependence while their numerical values are slightly different. The largest differences are observed for the zero wave-vector tracer diffusion coefficient that decreases by approximately 30% while its relaxation times increase by 15%.

Anisotropy of SISF is reflected by the lattice geometry function  $\eta(\mathbf{k})$  and the wave-vector orientation dependence of the parameters, especially the scaling parameter  $\kappa$ . The hydrodynamic limit of  $D_{s0}(t)$  correlates well with the results of Monte Carlo simulation of the particle mean-square displacements.

\*loukas@kelifos.physics.auth.gr

†panos@physics.auth.gr

<sup>1</sup>L. Onsager, *Phys. Rev.* **65**, 117 (1944).

<sup>2</sup>M. E. Fisher, *The Nature of Critical Points* (University of Colorado Press, Colorado, 1965).

<sup>3</sup>R. J. Baxter, *Exactly Solved Models in Statistical Mechanics* (Academic Press, London, New York, 1982).

<sup>4</sup>R. Gomer, *Rep. Prog. Phys.* **53**, 917 (1990).

<sup>5</sup>M. C. Tringides and Z. Choj, eds., *Collective Diffusion on Surfaces: Correlation Effects and Adatom Interaction*, NATO Science Series II. Mathematics, Physics and Chemistry, Vol. 29 (Kluwer Academic Press, Dordrecht, The Netherlands, 2001).

<sup>6</sup>A. R. Allnatt and A. B. Lidiard, *Atomic Transport in Solids* (Cambridge University Press, Cambridge, 2004).

<sup>7</sup>W. R. McKinnon and R. R. Haering, *Modern Aspects in Electrochemistry* (Plenum Press, New York, 1983).

<sup>8</sup>M. D. Levi and D. Aurbach, *Electrochim. Acta* **45**, 185 (1999).

<sup>9</sup>J. Bisquert, *Phys. Chem. Chem. Phys.* **10**, 49 (2008).

<sup>10</sup>A. A. Chumak and A. A. Tarasenko, *Surf. Sci.* **91**, 694 (1980).

<sup>11</sup>V. P. Zhdanov, *Surf. Sci.* **149**, L13 (1985).

<sup>12</sup>M. Tringides and R. Gomer, *Surf. Sci.* **166**, 419 (1986).

<sup>13</sup>H. Spohn, *Large Scale Dynamics of Interacting Particles* (Springer, New York, 1991).

<sup>14</sup>A. Danani, R. Ferrando, and E. Scalas, *Int. J. Mod. Phys. B* **11**, 2217 (1997).

<sup>15</sup>D. Zubarev, V. Morozov, and G. Repke, *Statistical Mechanics of Nonequilibrium Processes* (Akademie Verlag, Berlin, 1996), Vol. 1; (Akademie Verlag, Berlin, 1997), Vol. 2.

<sup>16</sup>R. Zwanzig, *Nonequilibrium Statistical Mechanics* (Oxford University Press, Oxford, 2001).

<sup>17</sup>G. S. Bokun, Ya. G. Groda, C. Uebing, and V. S. Vikhrenko, *Physica A* **296**, 83 (2001).

<sup>18</sup>P. Argyrakis, Y. G. Groda, G. S. Bokun, and V. S. Vikhrenko, *Phys. Rev. E* **64**, 066108 (2001).

<sup>19</sup>J. P. Boon and S. Yip, *Molecular Hydrodynamics* (McGraw-Hill International, New York, 1980).

<sup>20</sup>J. P. Hansen and I. R. McDonald, *Theory of Simple Liquids* (Academic Press, London, 1986).

- <sup>21</sup>P. A. Egelstaff, *An Introduction to the Liquid State* (Clarendon Press, Oxford, 1994).
- <sup>22</sup>P. Grosfils, J.-P. Boon, and P. Lallemand, *Phys. Rev. Lett.* **68**, 1077 (1992).
- <sup>23</sup>P. Grosfils, J.-P. Boon, R. Brito, and M. H. Ernst, *Phys. Rev. E* **48**, 2655 (1993).
- <sup>24</sup>G.-P. Rivert, J.-P. Boon, *Lattice gas hydrodynamics* (Cambridge University Press, Cambridge, 2001).
- <sup>25</sup>R. Blaak and D. Dubbeldam, *J. Stat. Phys.* **108**, 283 (2002).
- <sup>26</sup>R. Kutner, *Phys. Lett. A* **81**, 239 (1981).
- <sup>27</sup>R. Kutner and K. W. Kehr, *Phys. Rev. B* **41**, 2784 (1990).
- <sup>28</sup>E. H. Feng and H. C. Andersen, *J. Chem. Phys.* **121**, 3598 (2004).
- <sup>29</sup>R. Ferrando, R. Spadacini, and G. E. Tommei, *Phys. Rev. E* **48**, 2437 (1993).
- <sup>30</sup>G. Caratti, R. Ferrando, R. Spadacini, and G. E. Tommei, *Chem. Phys.* **235**, 157 (1998).
- <sup>31</sup>E. Arapaki, P. Argyrakis, and M. C. Tringides, *Phys. Rev. B* **62**, 8286 (2000).
- <sup>32</sup>P. A. Fedders and O. F. Sankey, *Phys. Rev. B* **18**, 5938 (1978).
- <sup>33</sup>R. A. Tahir-Kheli and R. J. Elliott, *Phys. Rev. B* **27**, 844 (1983).
- <sup>34</sup>R. A. Tahir-Kheli, *Phys. Rev. B* **27**, 6072 (1983).
- <sup>35</sup>H. van Beijeren and R. Kutner, *Phys. Rev. Lett.* **55**, 238 (1985).
- <sup>36</sup>C. T. Chudley and R. J. Elliott, *Proc. Phys. Soc. London* **77**, 353 (1961).
- <sup>37</sup>P. A. Egelstaff, *Adv. Phys.* **11**, 203 (1962).
- <sup>38</sup>M. Bee, *Chem. Phys.* **292**, 121 (2003).
- <sup>39</sup>O. Sobolev, L. L. Forestier, M. A. Gonzalez, M. Russina, E. Kemner, G. J. Cuello, and L. Charlet, *J. Phys. Chem. C* **113**, 13801 (2009).
- <sup>40</sup>J. Frenkel, *Kinetic Theory of Liquids* (Oxford University Press, Oxford, 1947).
- <sup>41</sup>G. S. Bokun, Ya. G. Groda, C. Uebing, and V. S. Vikhrenko, *Physica A* **296**, 83 (2001).
- <sup>42</sup>E. H. Feng and H. C. Andersen, *J. Chem. Phys.* **121**, 3582 (2004).
- <sup>43</sup>S. Chandrasekhar, *Rev. Mod. Phys.* **15**, 1 (1943).
- <sup>44</sup>A. Serra and R. Ferrando, *Surf. Sci.* **515**, 588 (2002).